

Nonlinear optical properties of antimony–germanium–sulfur glasses at 1560 nm

L.A. Gómez · C.B. de Araújo · R. Putvinskis Jr. ·
S.H. Messaddeq · Y. Ledemi · Y. Messaddeq

Received: 25 August 2008 / Published online: 1 November 2008
© Springer-Verlag 2008

Abstract Nonlinear (NL) optical properties of antimony–germanium–sulfur (Sb–Ge–S) glasses were investigated using laser pulses of 65 fs at 1560 nm. Samples having concentration ratio $[S]/[Ge] = 2.69$ with different antimony concentrations were studied. Glasses with different oxidation states of Sb were investigated using the *thermally managed Z-scan technique*. The influence of the Sb oxidation state on the NL properties was evaluated. NL refraction indices of electronic origin, $n_2 \approx 10^{-13} \text{ cm}^2/\text{W}$, two-orders of magnitude larger than for fused silica and NL absorption coefficients smaller than 0.55 cm/GW were measured. Appropriate figures-of-merit for photonic applications were determined.

PACS N.42.65.An · 42.70.-a · 42.70.Ce · 78.20.-e · 78.20.Ci

1 Introduction

Chalcogenide glasses are attracting the attention of many investigators due to their large transparency in the infrared, their high refractive index, and low phonon energies that make them good candidates for photonic applications [1–13]. Compositions based on tellurium [6], antimony–sulfide [7], and arsenium–sulfide [8, 9], among others [3–5,

10–13], have been studied aiming possible photonic applications. A glass family of interest is the ternary composition antimony–germanium–sulfur (Sb–Ge–S) that presents high nonlinear (NL) refraction index, n_2 . Changes in n_2 by $\approx 400\%$ were observed in the system $x\text{GeS}_2-(1-x)\text{Sb}_2\text{S}_3$, varying x from 10 to 40% [13]. Substitution of S by selenium (Se) in the system $\text{Ge}_{0.23}\text{Sb}_{0.07}\text{S}_{0.70-x}\text{Se}_x$ for x varying from 0 to 70% changed n_2 from 1.66×10^{-14} to $10.3 \times 10^{-14} \text{ cm}^2/\text{W}$ in experiments using a laser operating at 1064 nm (pulses of 15 ps). Two-photon absorption coefficients, $\alpha_2 < 0.1 \text{ cm/GW}$, were observed for some compositions [13]. The figure-of-merit, $T = 2\alpha_2\lambda/n_2$, where λ is the laser wavelength, was calculated, and values of $T < 1.1$ were obtained for small Se concentration ($x < 0.2$). The results indicate that this material may present good performance in devices such as directional couplers and NL distributed feedback gratings that require $T < 1$ and $T < 4$, respectively [14].

We report here on NL optical properties of Sb–Ge–S glasses at 1560 nm, a telecom wavelength. The influence of the antimony's states of oxidation was investigated for samples having concentration ratio $[S]/[Ge] = 2.69$, with [Sb] varying from 1 to 15%. Large NL refractive indices of electronic origin ($\approx 10^{-13} \text{ cm}^2/\text{W}$) and two-photon absorption coefficients smaller than 0.55 cm/GW were measured.

2 Experimental details

The glass compositions are presented in Table 1. High-purity GeS, S, and Sb with different oxidation states corresponding to Sb_2S_3 , Sb_2S_5 , and Sb^0 raw materials were mixed in 10 g into fused quartz ampoules in an N_2 gas-filled glove box with concentration of H_2O and O_2 smaller than 1 ppm. The sealed ampoule was held at 500°C for 3 h to

L.A. Gómez · C.B. de Araújo (✉)
Departamento de Física, Universidade Federal de Pernambuco,
50670-901 Recife, PE, Brazil
e-mail: cid@df.ufpe.br

R. Putvinskis Jr. · S.H. Messaddeq · Y. Ledemi · Y. Messaddeq
Instituto de Química, UNESP, 14801-970 Araraquara, SP, Brazil

Table 1 Compositions and parameters for the samples studied. n_0 is the linear refraction index at 1550 nm, n_2 is the NL refraction index in cm^2/W , and α_2 is the NL absorption coefficient in cm/GW

Sample	Composition	Acronym	n_0	$n_2 \times 10^{-14}$	α_2
A	2Sb ₂ S ₃ –26GeS–38S	Sb ₄ Ge ₂₆ S ₇₀	2.1102	6.54 ± 1.47	<0.43
B	2Sb ₂ S ₅ –26GeS–34S	Sb ₄ Ge ₂₆ S ₇₀	2.1435	6.57 ± 0.61	<0.24
C	4 Sb ₂ S ₅ –24.9GeS–22.2S	Sb ₈ Ge _{24.9} S _{67.1}	2.1578	7.18 ± 0.61	0.55

assist the reaction between Ge and S and then melted completely at 850°C during 10 h.

To increase the homogeneity of the melt, a rocking furnace was used. The melts were cooled in air for a few seconds, and the samples obtained were annealed during 4 h at 20°C, below the glass transition temperature, T_g . The final glass compositions, determined by energy dispersive spectroscopy (EDS), were the same as the initial composition within the accuracy of the measurement (2%). The values of T_g varying from $297 \pm 12^\circ\text{C}$ to $337 \pm 12^\circ\text{C}$ were determined using differential scanning calorimetry. The measurements were made with powdered samples placed in aluminum pans under N₂ atmosphere at heating rate of 10°C/min.

The samples used for the optical experiments have a disk shape with 10 mm diameter and 1 mm thickness.

Absorption spectra were obtained from 400 to 2000 nm using a double-beam spectrophotometer, and measurements of the linear refraction indices were made using the M-line technique at 1550 nm. For the NL measurements at 1560 nm, a mode-locked erbium-doped fiber laser delivering pulses of 65 fs at 50 MHz was used.

The NL measurements were made using the *thermally managed Z-scan* (TM-Z scan) *technique* [15]. This technique, a variation of the conventional Z-scan technique [16], allows differentiation between cumulative effects of thermal origin and the fast electronic nonlinearity, even when high-repetition-rate pulse trains are used. A chopper is the new element introduced in the conventional Z-scan setup, responsible for the thermal management as described in [15]. The method consists in acquiring the time evolution of the Z-scan signal for the sample positioned in prefocal and postfocal positions with respect to the region where the laser is focused. The time resolution of the measurement is determined by the chopper opening time ($t = 0$). The evolution of the Z-scan signal is obtained by delaying the photodetector signal acquisition time with respect to the chopper opening time. Then, the Z-scan curves can be constructed, and the contribution of thermal and electronic nonlinearities can be inferred using the procedures presented in [15, 16].

3 Results and discussion

Figure 1 shows the linear absorption coefficient, α_0 , for all samples prepared using Sb⁰ [Fig. 1(a)], Sb₂S₃ [Fig. 1(b)],

and Sb₂S₅ [Fig. 1(c)] with different concentrations of Sb. The results show band gap wavelengths in the range from ≈ 500 to ≈ 700 nm and a transparency window which extends to the infrared region. The samples prepared using Sb⁰ present the highest transparency in the green-red region. A dependence of the optical bandgap versus the antimony content is understood considering that the binding energy of Sb–S bonds is much lower than that of the Ge–Sb bonds [17, 18].

The laser beam was focused with a 5 cm focal-length lens, and the intensity obtained in the focus was 248 MW/cm². The opening time of the chopper was 20 μs . The temporal response at each position of the sample was recorded using a program which simultaneously acquires data from an oscilloscope and controls the motor responsible for the sample position. For the *closed aperture Z-scan scheme*, measurements of the normalized transmittance in the prefocal and postfocal positions are used to obtain the maximum difference between the signal in the peak and in the valley (ΔT_{P-V}) as a function of time. Beam self-focusing/defocusing were not observed for the samples prepared using Sb⁰ even with the highest concentration of Sb (15%); the same occurred for the other samples doped with 1% of Sb. Three samples were available for the NL experiments as indicated in Table 1, and typical TM-Z scan curves in the *closed aperture scheme* at different times are shown in Fig. 2 for the samples containing 4% of Sb.

To compensate the undesired linear scattering contribution and to test the photo-stability of the samples, sequential measurements were made in three regimes of intensity (low, high and low), and the results were compared in order to check for structural changes. The results show changes only in the samples prepared from Sb⁰ indicating the absence of photo-darkening or photo-bleaching in the other samples.

The values of ΔT_{P-V} obtained as a function of time are shown in Fig. 3. Extrapolating the results towards $t = 0$, it is possible to determine the nonthermal contribution to n_2 that is calculated using the expression $n_2 = \lambda \Delta T_{P-V}(t = 0) / 0.812\pi L_{\text{eff}} I$, where $L_{\text{eff}} = (1 - \exp(-\alpha_0 L)) / \alpha_0$ is the effective length of the sample, L is the sample length, and I is the laser intensity.

TM-Z scan results corresponding to the *open aperture scheme* were observed only for sample C, and the variations of the normalized transmittance at $z = 0$ (ΔT) were measured as a function of time. Also extrapolating the results to

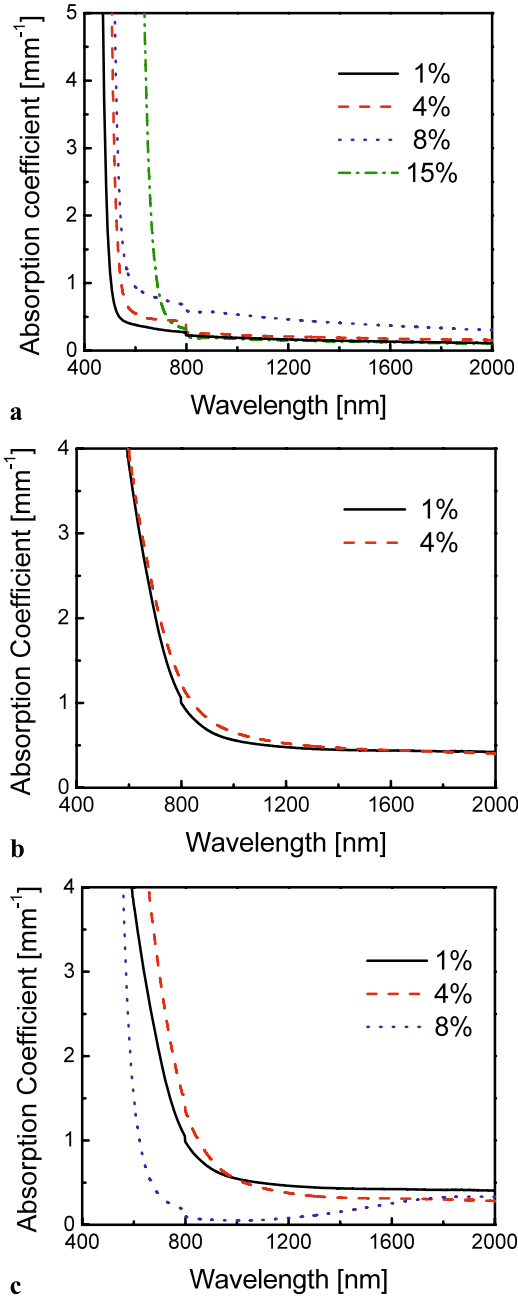


Fig. 1 Absorption spectra for samples prepared using (a) Sb^0 , (b) Sb_2S_3 , and (c) Sb_2S_5 with different concentrations of Sb

$t = 0$, we obtain the two-photon absorption coefficient using the expression $\alpha_2 = 2^{3/2} \Delta T(t = 0) / I L_{\text{eff}}$.

The results are summarized in Table 1. Note that high NL refractive indices of $\approx 10^{-13} \text{ cm}^2/\text{W}$ were determined for $t = 0$. The values of n_2 , attributed to the high polarizability of S and Sb, are much larger than for silica at 1550 nm ($n_2 = 2.87 \times 10^{-16} \text{ cm}^2/\text{W}$) [19]. The n_2 value for the glass $\text{Sb}_8\text{Ge}_{24.9}\text{S}_{67.1}$ [sample C] prepared from Sb_2S_5 are almost 500% higher than the values reported in [13] for $\text{Sb}_7\text{Ge}_{23}\text{S}_{70}$ and $\text{Sb}_{12}\text{Ge}_{23}\text{S}_{65}$ prepared from Sb_2S_3 . For

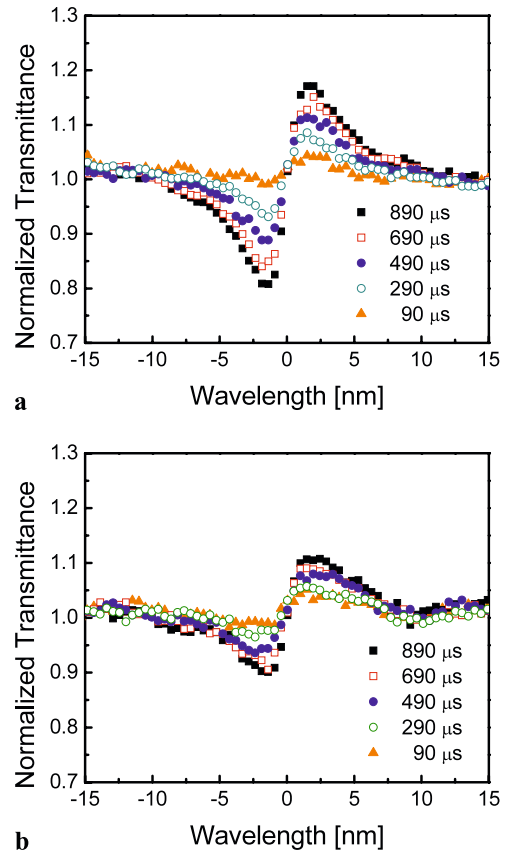


Fig. 2 Temporal evolution of the TM-Zscan curves in the closed aperture scheme for the sample doped with 4% of Sb and prepared with (a) Sb_2S_3 [sample A] and (b) Sb_2S_5 [sample B]

samples A and B, the open aperture transmittance ΔT is smaller than our limit of detection. Then, to estimate the value of α_2 , it was considered $\Delta T = 0.003$ at $t = 0$, which corresponds to the minimum NL transmission change that can be detected in our setup.

For the figure-of-merit $T = 2\alpha_2\lambda/n_2$, determined using the n_2 and α_2 values given in Table 1, we obtained $0.77 < T < 1.61$. However, for the samples prepared using Sb_2S_3 as precursor, a realistic estimate of T can be done assuming $\alpha_2 < 0.1 \text{ cm}^2/\text{GW}$, as reported in [13] for 1064 nm. This is justified because at 1560 nm, the linear absorption coefficient of the samples is comparable with the value at 1064 nm. In this case we obtain $T < 0.35$.

4 Summary

In summary, linear and NL optical properties of Sb–Ge–S were studied for samples prepared with different oxidation states of Sb. The NL response of the samples prepared from Sb^0 raw material was smaller than our limit of detection, while the samples prepared from Sb_2S_5 and Sb_2S_3 presented high NL refractive indices and low NL absorption

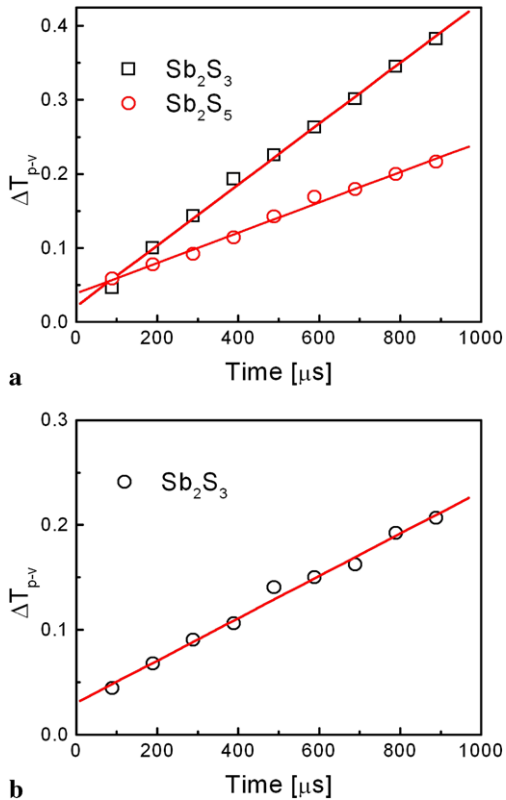


Fig. 3 ΔT_{p-v} for samples prepared using Sb_2S_3 and Sb_2S_5 with different concentrations of Sb: (a) 4%, (b) 8%

coefficients at 1560 nm. The measurements lead to figures-of-merit that indicate a large potential of the glasses studied for photonic applications at 1560 nm.

Acknowledgements We acknowledge financial support from Conselho Nacional de Desenvolvimento Científico e Tecnológico (CNPq) and Fundação de Amparo à Ciência e Tecnologia do Estado de Pernambuco (FACEPE). This work was performed under the Millennium Institute (Nonlinear Optics, Photonics and Bio-Photonics) Project and the Nanophotonics Network Program.

References

1. S.D. Jackson, G. Anzueto-Sánchez, *Appl. Phys. Lett.* **88**, 221106 (2006)
2. K. Ogusu, J. Yamasaki, S. Maeda, M. Kitao, M. Minakata, *Opt. Lett.* **29**, 265–267 (2004)
3. M. Yamane, Y. Asahara, *Glasses for Photonics* (Cambridge University Press, Cambridge, 2000)
4. A. Zakery, S.R. Elliott, *Optical Nonlinearities in Chalcogenide Glasses and their Applications*. Springer Series in Optical Sciences (Springer, Berlin, 2007)
5. A. Prasad, C.-J. Zha, R.-P. Wang, A. Smith, S. Madden, B. Luther-Davis, *Opt. Express* **16**, 2804 (2008)
6. J.C. Sabadel, P. Armand, D. Cachau-Herreillat, P. Baldeck, O. Doctot, A. Ibanez, E. Philippot, *J. Sol. State Chem.* **132**, 411 (1997)
7. C.B. de Araújo, G. Boudebs, V. Briois, A. Pradel, Y. Messaddeq, M. Nalin, *Opt. Commun.* **260**, 723 (2006)
8. J.M. Laniel, N. Hó, R. Vallée, A. Villeneuve, *J. Opt. Soc. Am. B* **22**, 437 (2005)
9. J. Troles, L. Brillanb, F. Smektala, N. Traynor, P. Houizot, F. De-sevedavy, In: *Proceedings of the International Conference on Transparent Optical Networks*, vol. 2, pp. 297–300 (2007)
10. M. Guignard, V. Nazabal, J. Troles, F. Smektala, H. Zeghlache, Y. Quiquempois, A. Kudlinski, G. Martinelli, *Opt. Express* **13**, 789–795 (2005)
11. E.L. Falcão-Filho, C.B. de Araújo, C.A.C. Bosco, G.S. Maciel, L.H. Acioli, M. Nalin, Y. Messaddeq, *J. Appl. Phys.* **97**, 013505 (2005)
12. L.A. Gómez, C.B. de Araújo, D.N. Messias, L. Misoguti, S.C. Zilio, M. Nalin, Y. Messaddeq, *J. Appl. Phys.* **100**, 116105 (2006)
13. L. Petit, N. Carlie, K. Richardson, A. Humeau, S. Cherukulappurath, G. Boudebs, *Opt. Lett.* **31**, 1495 (2006)
14. K.W. DeLong, K.B. Rochford, G.I. Stegeman, *Appl. Phys. Lett.* **55**, 1823 (1989)
15. A. Gnoli, L. Razzari, M. Righini, *Opt. Express* **13**, 7976 (2005)
16. M. Sheik-Bahae, A.A. Said, T.H. Wei, D.J. Hagan, E.W. Van Stryland, *IEEE J. Quantum Electron.* **26**, 760 (1990)
17. M.F. El-Sayed, *Opt. Laser Technol.* **38**, 14 (2006)
18. E. Márquez, T. Wagner, J.M. González-Leal, A.M. Bernal-Oliva, R. Prieto-Alcón, R. Jiménez-Garay, P.J.S. Ewen, *J. Non-Crystall. Solids* **274**, 62 (2000)
19. D. Milam, *Appl. Opt.* **37**, 546–550 (1998)